Research Square

Preprints are preliminary reports that have not undergone peer review.
They should not be considered conclusive, used to inform clinical practice,
or referenced by the media as validated information.

Resveratrol-loaded oil-in-water emulsion-based delivery systems: Impact of droplet size, pH, temperature, and ultraviolet light on stability

Adrian Boldianu
University of Massachusetts Amherst
David Julian McClements
mcclements@foodsci.umass.edu
University of Massachusetts Amherst

Research Article

Keywords: resveratrol, medium-chain triglycerides oil, droplet size, pH-driven loading, UV-light exposure, spatial partition

Posted Date: August 7th, 2026

DOI: https://doi.org/10.21203/rs.3.rs-10590835/v1

License: This work is licensed under a Creative Commons Attribution 4.0 International License.
Read Full License

Additional Declarations: No competing interests reported.

Resveratrol-loaded oil-in-water emulsion-based delivery systems: Impact of droplet size, pH, temperature, and ultraviolet light on stability

Adrian Bogdan Boldianu[1] and David Julian McClements[2]

[1]Department of Chemistry and Biochemistry, University of Agricultural Sciences and Veterinary Medicine, Mănăştur Street 3–5, 400372 Cluj-Napoca, Romania

[2]Biopolymers and Colloids Laboratory, Department of Food Science, University of Massachusetts, Amherst, MA 01003, USA

Contact Information: Professor David Julian McClements, Biopolymers and Colloids Laboratory, Department of Food Science, University of Massachusetts, Amherst, MA 01003, USA; mcclemen@umass.edu

Abstract

Resveratrol is a bioactive polyphenol with antioxidant and health-promoting activities, but its poor water solubility and chemical stability limit its use as a functional ingredient. This study explored the impact of droplet size, pH, storage temperature, and UV light exposure on the partitioning and stability of resveratrol loaded in medium-chain triglyceride (MCT) oil-in-water emulsions. Resveratrol was loaded into the oil droplets using a pH-driven method based on the substantial reduction in the water-solubility of resveratrol when the pH is adjusted from alkaline to neutral. Initially, oil droplets with different mean droplet diameters (D_{32}) were prepared by varying the homogenization method and operating conditions: small (0.62 μm), medium (1.29 μm), and large (6.79 μm). There was a slight increase in droplet size for the emulsions containing small droplets after incorporation of resveratrol. Moreover, the surface charge of small and medium droplets became more negative after resveratrol loading, suggesting some of it was located at the oil-water interface. The oil solubility, encapsulation efficiency, and oil/water partitioning of resveratrol were measured. The maximum solubility of resveratrol in MCT oil was 2.03 mg/mL at 37°C. The partitioning of resveratrol into the oil phase was highest (>74%) for the emulsions containing the smallest droplets. In general, the encapsulation efficiency of the resveratrol in the emulsions was relatively high (>93%), suggesting there was little loss of resveratrol during the loading process. All emulsions remained stable throughout 21 days storage at 4°C, with little resveratrol loss and little change in droplet characteristics. However, storage at 37°C caused some resveratrol degradation, especially in the emulsions containing the largest droplets. The resveratrol remained relatively stable when stored at pH values from 3 to 7 but exhibited appreciable degradation when stored at pH 8 and 9, highlighting the poor stability of this polyphenol under alkaline conditions. When exposed to UV light, resveratrol degradation followed second-order kinetics. The photostability of resveratrol was better when encapsulated in small oil droplets and stored under mildly acidic to neutral pH conditions (longer half-life) than when encapsulated in larger oil droplets and stored under alkaline pH values (shorter half-life). These findings show that resveratrol stability is enhanced by reducing oil droplet size and storing the emulsions under acidic or neutral pH conditions at refrigerated temperatures, offering practical guidance for the formulation of resveratrol-based functional foods and cosmeceuticals.

Keywords: resveratrol, medium-chain triglycerides oil, droplet size, pH-driven loading, UV-light exposure, spatial partition

1. Introduction

Resveratrol, a non-flavonoid polyphenolic compound, is a phytoalexin synthesized by plants, with a structure that consists of two benzene rings joined by an ethylene bridge, resulting in a stilbene backbone (Kasiotis et al., 2013). This bioactive compound has gained considerable scientific attention due to its diverse biological effects, including cardioprotective (Kasiotis et al., 2013), anti-inflammatory (Meng et al., 2021), antioxidative (Silva et al., 2023), and antineoplastic (Berman et al., 2017) properties. Moreover, it may be utilized in metabolic health management (Su et al., 2022), to modulate the tumor microenvironment (Talib et al., 2020), to enhance cognitive function (Shi et al., 2024), and to improve female fertility (Bertoldo et al., 2024).

Despite its therapeutic potential, resveratrol, similar to many other predominantly hydrophobic compounds, suffers from formulation and delivery problems associated with its poor water solubility and chemical instability when exposed to certain environmental conditions, such as heat, light, oxygen, and alkalis (Jiang et al., 2025). These limitations can compromise its bioavailability and bioactivity in biological systems, thereby reducing its efficacy. Encapsulation in emulsion-based delivery systems has, however, proven to be an effective method of improving the dispersibility, stability, and bioavailability of such compounds (Silva et al., 2023).

Initially, we aimed to evaluate how oil droplet size affects resveratrol's oil/water partitioning, encapsulation efficiency, and chemical stability using medium-chain triglyceride (MCT) oil-in-water emulsions as model systems. This information is valuable for the optimization of resveratrol-loaded emulsion formulations and understanding the contribution of droplet attributes to the behavior of encapsulated compounds under different environmental stressors. It was hypothesized that droplet size would influence the physical and chemical stability of the emulsions. MCT oil was used because it is mainly composed of medium-chain fatty acids (C8 - C12) (Nimbkar et al., 2022). In contrast to other vegetable oils, like olive, corn, or sunflower oils, MCT oil does not contain long-chain fatty acids, polyphenols, or other bioactive molecules that could interfere with resveratrol stability or confound our results by influencing oxidation reactions (Li et al., 2024; Taha et al., 2018). The use of MCT therefore facilitates the evaluation of resveratrol's behavior in emulsion systems.

The pH-driven loading method was used to introduce the resveratrol into pre-formed oil-in-water emulsions, as it has been shown to be a simple, inexpensive, and efficient method of incorporating

polyphenols into hydrophobic colloidal particles (B. Zheng et al., 2018). Indeed, this method has been shown to achieve high encapsulation efficiencies for a wide range of polyphenols (Zhou et al., 2024). The homogenization methods, surfactant type, and pH range used to formulate the emulsions were selected based on their suitability for practical applications. The high shear mixing, sonication, and microfluidization methods used to prepare emulsions with different droplet sizes are commonly used industrially (McClements, 2015). The surfactant used to form and stabilize the emulsions, Quillaja saponin, is a natural food-grade surfactant derived from a plant source (Reichert et al., 2019). The pH range (3–9) of the emulsions studied covers the broad range of values found in foods and beverages, including soft drinks (Reddy et al., 2016), fruit juices (Khan et al., 2025), and dairy alternatives (Daszkiewicz et al., 2024).

We hypothesized that variations in oil droplet size and pH would influence the chemical stability of the encapsulated resveratrol, as well as its partitioning between the oil and water phases in the emulsions. This hypothesis is based on the fact that the physical and chemical properties of emulsion systems greatly influence the behavior and stability of encapsulated molecules (Zhao et al., 2024; X. Zheng et al., 2025). The findings of this research may lead to the design and formulation of more stable and efficacious resveratrol delivery systems.

2. Materials and methods

2.1 Materials

Trans-resveratrol (R0071, purity >99%) was obtained from TCI America (Tokyo, Japan). Acetonitrile (HPLC grade) and acetic acid (>99.7%) were purchased from Thermo Fisher Scientific Inc. (Waltham, MA, USA). Pure MCT oil (MIGLYOL 812 N) was purchased from Warner Graham Company (USA). Ethanol (HPLC grade) was obtained from VWR International (Lutterworth, England). Quillaja saponin (Q-Naturale 200) was acquired from Ingredion Inc. (Westchester, IL). Double-distilled water was used for all the experiments and emulsion preparation.

2.2 Preparation of MCT oil-in-water emulsions

Oil-in-water emulsions were prepared with three different oil droplet sizes. An aqueous surfactant solution was first prepared by dissolving 1.11 % w/w Quillaja saponin in double distilled water. An initial emulsion was then created by blending 10 % w/w MCT oil with 90 % w/w Quillaja

saponin solution (1% w/w in final emulsion) using a hand homogenizer (BioHomogenizer 1281, Biospec Products, USA) for 2 min at 10,000 rpm. A 10% MCT oil-in-water emulsion containing large droplets ("L") was then prepared by blending the initial emulsion using a high-shear homogenizer (PRO250, PROScientific, USA) for 10 min at 25000 RPM. An emulsion containing medium droplets ("M") was created by sonicating the initial emulsion (FB505, Fisher Scientific, USA) for 8 min, on-time and off-time 5:1 (sec), at an amplitude of 70% and frequency of 20 kHz using a 1/2 inch probe. During sonication, the emulsion was placed in an ice bath and continuously stirred to avoid overheating. An emulsion containing small droplets ("S") was prepared by passing the initial emulsion through a high-pressure microfluidizer (M-110L, Microfluidics, USA) for three passes at 12000 psi.

2.3 Loading of resveratrol into emulsions

The resveratrol was loaded into the different emulsions using a pH-driven method described previously (Zhou et al., 2021a). An alkaline resveratrol solution (pH 12.5) was prepared by adding the powdered resveratrol into a 0.1 N sodium hydroxide solution. The resveratrol solution was then stirred at room temperature with a measured amount of emulsion. After less than 5 minutes of magnetic stirring, the resveratrol-loaded emulsion was adjusted to pH 6 and diluted to a 5% w/w oil concentration. The final added quantity of resveratrol in the emulsion was 0.1 mg/g.

2.4 Trans-resveratrol concentration determination

The resveratrol concentration in the samples was measured using a high-performance liquid chromatography (HPLC, Agilent 1100 series, Agilent Technologies Inc., USA) method. To quantify the resveratrol concentration, an acidic ethanol solution (1% acetic acid) was added in a 1:1 ratio to the emulsion and then vortexed for 10 s. The resveratrol was then extracted by centrifugation at 10,000 rpm for 30 min at room temperature. After centrifugation, the supernatant was collected and filtered (0.45 μm filter) before being injected into the HPLC instrument.

The extracts were separated using a C18 reverse-phase column (4.6 nm × 250 nm, 5 μm, Agilent) and detected by UV-Vis at 307 nm. The mobile phase was a 30:70 v/v combination of acetonitrile and 1% acetic acid with double distilled water. The flow rate was kept constant at 0.4 mL/min. The resveratrol concentration was then calculated using a calibration curve prepared using a known resveratrol acidic ethanol solution (R=0.996). All samples were analyzed twice to confirm optimal system function.

2.5 Selection of oil phase and resveratrol solubility

To determine the maximum potential loading capacity, we evaluated the solubility of resveratrol in MCT oil using a standard saturation method (Chen et al., 2023). An excess amount of resveratrol powder (5 mg) was dispersed by vortexing in 1 ml of MCT oil. The samples were then stored at 25℃ and 37℃ for 96 h under continuous agitation conditions using an incubated rotator (H2024, Benchmark Scientific, USA). In addition, some samples were stored at 4℃ in a refrigerator and manually shaken twice every day. Every 24 h, the samples were centrifuged at 5,000 rpm for 10 min, and aliquots were collected from the supernatant. All aliquots were diluted (1:1, v/v) with an acidic ethanol solution (1% acetic acid) and then filtered (0.45 μm filter). The resveratrol quantification was then performed using HPLC as described in the previous section.

2.6 Encapsulation efficiency and oil/water partition determination

The resveratrol encapsulation efficiency (EE) in the emulsions was determined using the following equation:

$$EE(\%) = \frac{C}{C_0} \times 100 \quad (1)$$

Here, C represents the concentration of resveratrol in the emulsion after preparation, while C_0 represents the original concentration used in the preparation procedure. All concentrations were determined using the HPLC method described in Section 2.4.

To quantify the resveratrol concentration in the water phase, the emulsion was centrifuged at 10,000 rpm for 30 min, and then the lower water phase was collected and transferred to a separate microcentrifuge tube. To guarantee that no oil droplets were present in the final aqueous phase, a second centrifugation was performed using the same conditions. The procedure for extracting resveratrol from the final water phase was the same as described above.

The oil/water partition of resveratrol in the emulsions was calculated as follows:

$$Resveratrol\ in\ water\ phase(\%) = \frac{C_{water}}{C_{total}} \times 100 \quad (2)$$

$$Resveratrol\ in\ oil\ phase(\%) = \frac{C_{droplet}}{C_{total}} \times 100 \quad (3)$$

The difference between the total concentration of resveratrol in the emulsion (C_{total}) and the concentration of resveratrol in the water phase (C_{water}) was taken to be the resveratrol concentration

in the oil droplets ($C_{droplet}$). In reality, the resveratrol concentration in the oil droplets includes resveratrol dissolved in both the oil phase and in the interfacial layer at the droplet surfaces.

2.7 Particle dimensions and surface potential

The surface-weighted mean diameter (D[3,2]) and particle size distribution (PSD) were assessed using a laser diffraction device (Mastersizer 3000, Malvern Instruments, Worcestershire, UK). Particle electrophoresis (Zetasizer Pro, Malvern Instruments) was used to assess the surface potential (ζ-potential) of loaded and unloaded emulsion samples. Prior to measurement, the 5% oil (w/w) emulsions were diluted 10 times with phosphate buffer solution (PBS, 5 mM, 68.5 mM sodium chloride) of the same pH (pH 6.0). To reach the same final droplet concentration, the 10% oil (w/w) samples were diluted 20 times with the same phosphate buffer solution. To avoid dilution-induced artifacts and to ensure comparability, the surface charge was measured after diluting the emulsions in PBS buffer with a fixed ionic strength of 68.5 mM. This concentration was selected as the minimum salinity required to stabilize the pH at 6.0 and provide adequate conductivity for zeta potential analysis (Bonto et al., 2019).

2.8 Microstructure

The microstructure of resveratrol-loaded emulsions was analyzed using a confocal laser scanning microscope (CLSM, Nikon, D-Eclipse C1 80i, NY). The samples were stained by adding a Nile Red ethanol solution (1 mg/mL) in a 1:10 ratio (v/v) to the emulsions. The dyed emulsions were then placed on a microscope slide, covered with a coverslip, and examined using a 40× objective lens. The images were acquired using the microscope's digital camera and then stored and analyzed using the instrument software.

2.9 Storage and pH stability

All resveratrol-loaded emulsions were stored at 4℃ and 37℃ for 21 days. Their stability was assessed immediately after resveratrol loading (day 0), and then after 9, 15, and 21 days of storage. All samples were shaken at least once per day. Information about their storage stability was obtained using several methods: change in particle size parameters by laser diffraction; phase separation perception by digital photography; microstructure change by confocal microscopy; resveratrol concentration and oil/water partition by extraction and HPLC analysis.

An emulsion containing small oil droplets was freshly prepared, separated into different test tubes, and then their pH values were adjusted to pH 3, 5, 7, 8, and 9 using sodium hydroxide and hydrochloric acid solutions. The samples were then stored at 4℃ and 37℃ for 21 days, and their stability was assessed after 0, 3, 5, 10, 15, and 21 days as described previously.

2.10 UV-light stability

The stability of resveratrol to light-induced degradation was tested in an accelerated UV-light exposure experiment utilizing a UV-light lamp (Blak-Ray UV, Ted Pella Inc., USA). A volume of 11 mL of each sample was placed in a Petri dish (60 mm diameter) and exposed to UV radiation at 365 nm for 2 h. Aliquots were obtained at 5, 10, 20, 40, 60, 90, and 120 minutes. Resveratrol was extracted and quantified from all aliquots using HPLC. The distance between the sample and the UV lamp bulb was fixed at 25 cm, and the intensity of the UV-light reported by the manufacturer was 8900 μW/cm². During the UV-light exposure time, the temperature was monitored using a handheld thermal camera (FLIR TG165-X, Teledyne FLIR LLC, USA) to ensure excessive heating did not promote extensive moisture evaporation or resveratrol degradation.

The degradation rate constants were determined by fitting a second-order kinetic model to the measured concentration-time data. For all pH values, the second-order model showed the highest correlation coefficient (highest R^2 among all tested models). Initially, a linear regression plot of reciprocal concentration ($1/C$) versus time (t) was constructed. Then, the second-order rate constant (k_2) was calculated from the slope of the linear regression (Ho, 2006):

$$\frac{1}{\mathrm{C}} = \frac{1}{\mathrm{C_0}} + k_2 t \quad (4)$$

Where, C is the resveratrol concentration at a given time point and $\mathrm{C}_o$is the initial concentration (100%). The half-life (t_{50}) during UV-light exposure was calculated using (Q. Hu & Zhang, 2020):

$$t_{50} = 1/(k_2 \times \mathrm{C_0}) \quad (5)$$

2.11 Statistical analysis

Each experiment included three independent biological replicates, and all samples were analyzed at least twice to ensure accurate readings. Data is presented as the mean ± standard error of the mean. All statistical analyses were conducted using JASP software (Version 0.19.3.0, RRID: SCR_015823).

In stability studies where aliquots of the same emulsion sample were analyzed repeatedly at successive time points, a repeated measures ANOVA (RM-ANOVA) was applied, followed by Bonferroni-adjusted pairwise comparisons for *post hoc* testing. In the case of comparison of different parameters within various conditions or formulations of interest (*e.g.,* droplet size or pH), one-way ANOVA was utilized. Student's t-tests were used to compare values measured before and after a treatment or experimental condition (e.g., pre- and post-UV exposure). For all tests, a p-value < 0.05 was considered statistically significant.

3. Results and discussion

3.1 Resveratrol solubility in MCT oil

Initially, the maximum amount of resveratrol that could be solubilized in the oil phase was determined as it influences the maximum amount of this bioactive compound that can be successfully loaded into an emulsion. In general, the water solubility of the resveratrol increased with increasing temperature, which may be due to higher entropy of mixing effects ($T\Delta S$), as well as alterations in water structure at elevated temperatures. The system appeared to have almost reached equilibrium after 24 h at each storage temperature, as there was not much change in the measured solubility afterwards. However, there did appear to be a slight increase in solubility from 24 to 72 h, followed by a slight decrease from 72 to 96 h (but not significant). The initial increase may have been because equilibrium had not been fully reached after 24 h, whereas the later decrease may have been due to some chemical degradation of the resveratrol. The highest resveratrol solubility in MCT oil was found to be 2.032±0.006 mg/mL after 72 h storage at 37°C (Fig. 1). The obtained values fall within the low-to-mid range of previously published data (Chen et al., 2023; Hung et al., 2006; Kotta et al., 2021). Differences in reported solubility values may arise due to differences in experimental design and solute/solvent variability.

Resveratrol's solubility in MCT oil influences its encapsulation efficiency and stability in emulsions. A higher solubility within the oil phase would be expected to increase the molecule's partitioning into the oil droplets, thereby lowering exposure to the surrounding aqueous phase and minimizing degradation (Chen et al., 2023). Based on these results, 2 mg/ml of resveratrol in MCT oil was used to prepare the nutraceutical-loaded emulsions in the remainder of the studies.

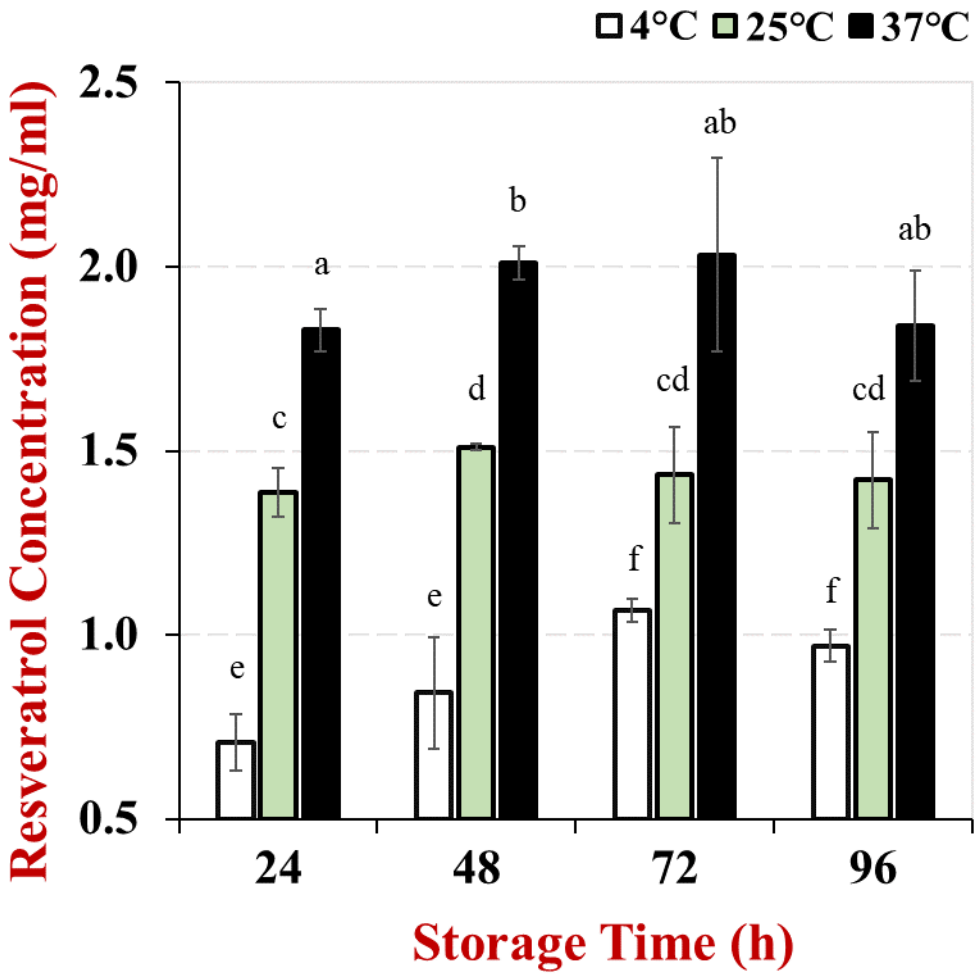


Figure 1: Resveratrol solubility in MCT oil measured at 4, 25, and 37°C over a 96-hour period. The soluble resveratrol concentration was measured after centrifugation of the samples to remove non-dissolved crystals.

3.2 Influence of the pH-driven resveratrol loading method on emulsion characteristics

Resveratrol-loaded MCT emulsions were successfully produced with three different lipid droplet sizes: small, medium, and large. The characteristics of these emulsions were analyzed before and after loading the resveratrol to assess the influence of the pH-driven loading protocol.

3.2.1. Droplet charge

Initially, all of the emulsions had a negative surface potential (ζ-potential), which can be attributed to the presence of deprotonated carboxyl groups on the Quillaja saponin [1]. Interestingly, the initial magnitude of the ζ-potential increased as the droplet size increased, rising from around -17 mV for the small droplets to around -32 mV for the large droplets (Figure 2A). After loading the resveratrol into the emulsions, the magnitude of the ζ-potential increased significantly for the emulsions containing small droplets (-17.15 ± 4.3 mV to -21.92 ± 0.79 mV) and medium droplets (-18.99 ± 3.0 mV to -22.7 ± 1.5 mV). In contrast, it remained largely unchanged for the emulsions containing large droplets (Figure 2A). For electrostatically stabilized emulsions, a larger ζ-potential typically leads to a greater resistance to aggregation, since then there is a stronger electrostatic repulsion between the oil droplets (Miadonye & Amadu, 2023). This can enhance the long-term physical stability of emulsions by reducing droplet flocculation and coalescence. However, other stabilization mechanisms, such as steric repulsion, may also impact the resistance of the emulsions to aggregation.

3.2.2. Droplet size

The initial mean droplet diameters (D[3,2]) of the small, medium, and large emulsions were 0.62 ± 0.01, 1.29 ± 0.03, and 7.79 ± 0.03 μm (Figure 2B), respectively, indicating that the different homogenization methods used were capable of forming emulsions with a range of different droplet sizes. After loading, the average droplet diameter increased from 0.62 ± 0.01 μm to 0.69 ± 0.01 μm for the emulsion containing the small droplets ($p < 0.05$). In contrast, there was no significant change in the droplet size for the emulsions containing medium or large droplets. The particle size distribution profiles also showed that there was little change in the droplet size characteristics for the emulsions containing medium or large droplets but a slight change in the ones containing small droplets (Figure 2C, 2D, 2E).

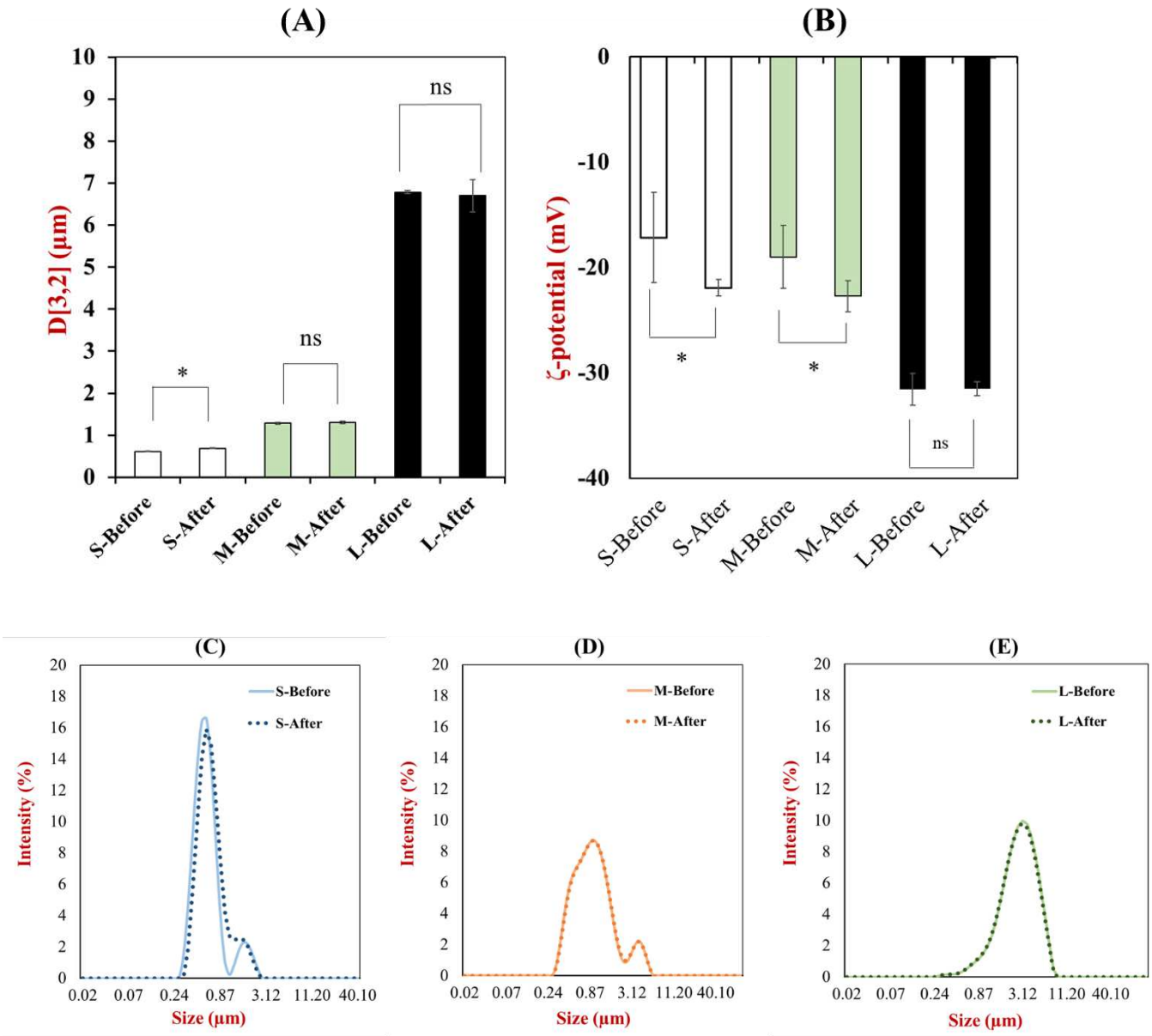


Figure 2: Characteristics of emulsions containing small, medium, and large (S, M, and L) droplets before and after resveratrol loading: **(A)** surface charge, **(B)** surface area mean diameter (D[3,2]), **(C)** particle size distribution for the small size droplet emulsion, **(D)** particle size distribution for the medium size droplet emulsion, **(E)** particle size distribution for the large size droplet emulsion. *$p < 0.05$

The fact that an increase was only seen in the emulsion containing the smallest droplets may have been because it had the largest specific surface area and smallest dimensions (Ten Klooster et al.,

2024). As a result, any resveratrol located at the oil-water interface may have had a larger impact on the measured particle size. Indeed, previous studies have reported that resveratrol does have a tendency to partition to the oil-water interfaces of emulsion systems (Losada-Barreiro et al., 2014). In general, the size of the droplets in an emulsion impacts both their physical and chemical stability (Golding & Wooster, 2010; Li & McClements, 2010). For instance, faster droplet aggregation and creaming typically occur in emulsions containing larger oil droplets, leading to more rapid physical destabilization. The chemical stability of an encapsulated bioactive may also depend on the droplet size and surface area, as this influences its exposure to the surrounding aqueous phase (Kharat et al., 2020). Consequently, it is often important to optimize the droplet size characteristics for each application.

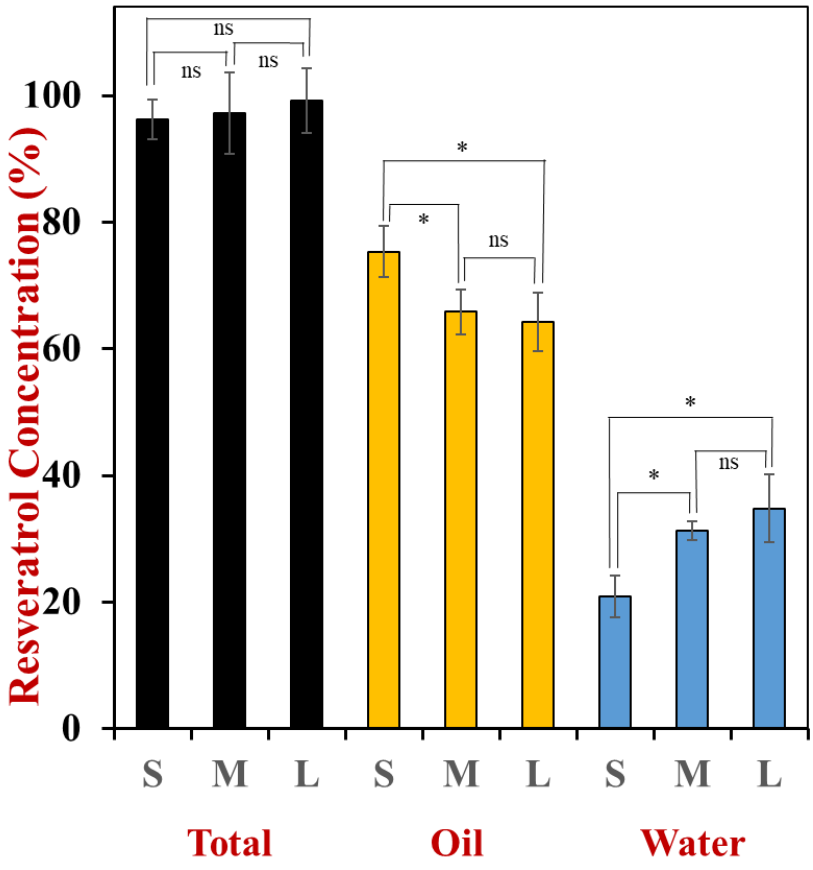


Figure 3: Resveratrol partitioning between aqueous phase (AP) and oil phase (OP) after the pH-driven loading method for emulsions containing small, medium, and large (S, M, and L) droplets. Key: significant differences marked by * ($p < 0.05$).

3.2.3. Resveratrol partitioning

The location of polyphenols within emulsions, such as the relative proportions in the oil, water, and interfacial regions, can impact their chemical stability, as this influences the molecules within their local environment [2]. The influence of lipid droplet size on resveratrol partitioning between the oil and aqueous phases was therefore evaluated in the emulsions containing small, medium, and large droplets (Fig. 3). Notably, the oil phase here actually consists of the oil droplet interior and the interfacial regions. The total amount of resveratrol measured in all the emulsions was slightly less than 100%, ranging from around 96% to 99%, which may have been due to some losses or chemical degradation of the polyphenols during emulsion preparation. The fraction of resveratrol in the oil phase (64.3-75.1%) was appreciably higher than that in the aqueous phase (20.9-34.8%), even though the oil phase only made up about 5% of the total emulsion, which can be attributed to the fact that resveratrol is a relatively hydrophobic molecule. The percentage of resveratrol in the oil phase increased as the droplet size decreased, whereas the percentage in the aqueous phase decreased (Fig. 3). This effect may have been because some of the resveratrol was associated with the interfacial region at the oil droplet surfaces, and there was a larger specific surface area for the emulsions containing the smallest droplets (Meynier et al., 2005).

In general, the distribution of substances between oil and water phases is determined by the equilibrium partition coefficient (K_{OW}), which is the concentration in the oil phase divided by the concentration in the water phase after equilibrium is attained. The K_{OW} of resveratrol has been reported to be around 1260, *i.e.,* logP = 3.1 (Robinson et al., 2015). To a first approximation, the K_{OW} values can be calculated from the relative concentrations of resveratrol in the oil and water phases (%O and %W), as well as the relative volume fractions of the oil and water phases (ϕ_O = 0.05 and ϕ_W = 0.95) using the following expression:

$$K_{OW} = \frac{\%O}{\%W} \times \frac{\phi_W}{\phi_O} \quad (6)$$

This calculation gave values of K_{OW} of 68.4, 40.0, and 35.1 for the emulsions containing the small, medium, and large droplets, respectively. Notably, these values are considerably smaller than the one reported in the literature, *i.e.,* there is less in the oil phase that expected. This discrepancy may have been partly because the literature K_{OW} value is for octanol-water partitioning, whereas in our study the measurements were made for MCT-water partitioning (Chen et al., 2023). Moreover,

the presence of any Quillaja saponin micelles in the aqueous phase may have altered the partitioning of the resveratrol between the two phases, as micelles can solubilize hydrophobic substances like polyphenols in their hydrophobic cores (Cvejić et al., 2014). Overall, the resveratrol partitioning results found in our study are consistent with those reported in prior studies (Zhou et al., 2021a).

3.3 Storage stability

For commercial applications of delivery systems, it is important that they remain stable during storage. For this reason, changes in the physical and chemical stability of the resveratrol-loaded emulsions were monitored during storage under different temperature conditions.

3.3.1 Impact of droplet size on droplet characteristics and resveratrol stability and partitioning

The mean droplet diameters of all three emulsions (small, medium, and large) remained relatively constant during storage at 4°C and 37°C for 21 days (Table 1). Macroscopic observations (Fig. 4A) and microstructure monitoring (Fig. 4B) were also used to provide insights into changes in the physical stability of the different emulsions during storage. The emulsion containing the large droplets showed visible creaming during storage, however the droplets could be readily redispersed upon gentle agitation without any change in their size. These results suggest that the large oil droplets were susceptible to creaming, which can be attributed to the stronger gravitational forces acting on these droplets. However, they were resistant to aggregation (flocculation and coalescence), which can be attributed to the strong steric and electrostatic repulsion provided by the Quillaja saponin adsorbed to their surfaces. The emulsions containing small and medium droplets were resistant to both creaming and aggregation, which can be attributed to their smaller sizes leading to weaker gravitational forces.

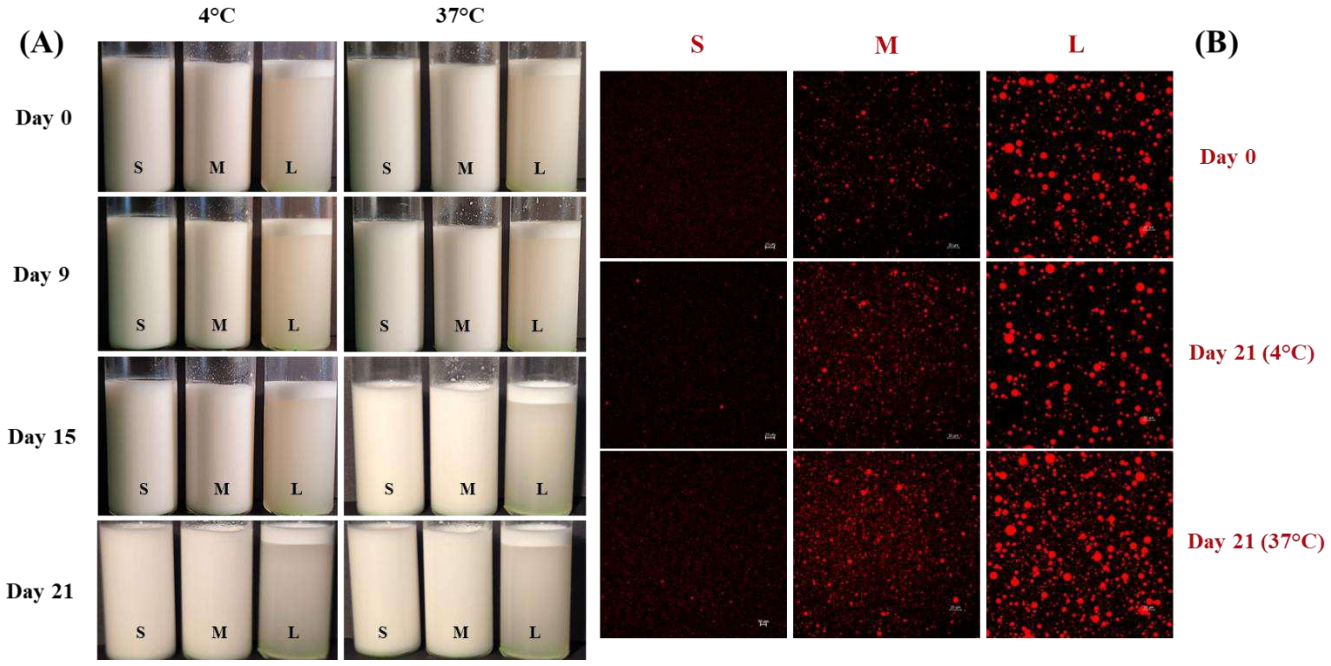
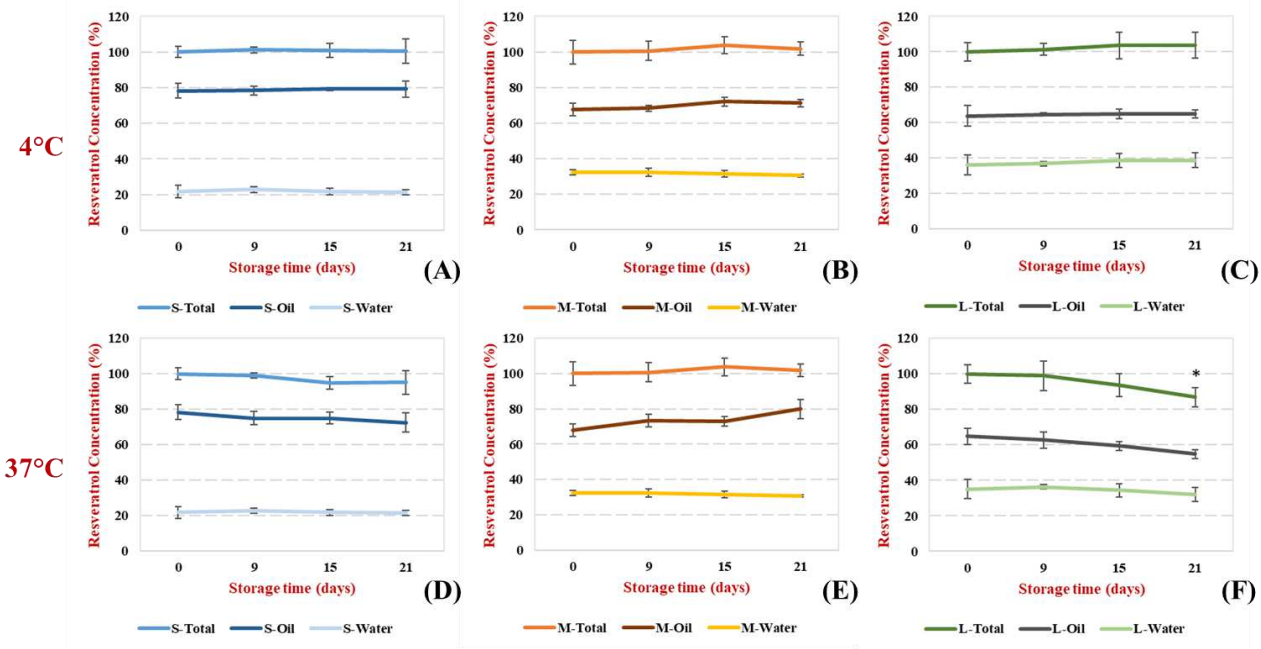


Figure 4: Emulsion characteristics representing macroscopic aspect **(A)** and microstructure **(B)** before and after 21 days of storage at 4°C and 37°C.

There were some changes in the electrical characteristics of the oil droplets in the emulsions during storage, but the magnitude of this effect depended on droplet size. The emulsions containing the small droplets exhibited negligible surface charge changes (Table 1), while the ones containing medium droplets showed a significant ζ-potential shift during storage at 37°C ($p < 0.05$). The ζ-potential value for the emulsions containing the large droplets changed from -32.60 ± 0.67 mV initially to -30.11 ± 0.28 mV at 4°C and -26.23 ± 1.23 mV at 37°C ($p < 0.001$) after 21 days of storage. Thus, there was a decrease in the magnitude of the ζ-potential values in some emulsions during storage, especially at the higher storage temperature. This effect suggests that there may have been some chemical changes in the interfacial layers of the oil droplets during storage, such as cleavage of carboxyl groups on the saponins (McClements, 2015; Ulaganathan et al., 2019).



380

381 **Figure 5**: Measured and calculated resveratrol concentration (%) during the 21 days of storage
382 time. The included data shows the concentration from the entire emulsion (Total), the aqueous
383 phase (Water), and the oil and surfactant phase (Oil). Emulsions with small (S), medium (M), and
384 large (L) droplet sizes were evaluated. The storage temperature was represented by 4°C **(A, B, C)**
385 and 37°C **(D, E, F).** *p<0.05

386

387 **Table 1**: Surface potential (ζ-potential) and mean particle diameter (D [3,2]) before and after 21
388 days storage at 4 and 37°C for emulsions containing small (S), medium (M) and large (L) oil
389 droplets. Values are expressed as mean ± standard deviation from at least three biological
390 replicates. *p<0.05, **p<0.01, ***p<0 .001

Storage time	*Day 0*		*Day 21 (4°C)*		
Sample	ζ-potential (mV)	D [3,2] (μm)	ζ-potential (mV)	D [3,2] (μm)	ζ-
S	-22.88 ± 0.71	0.689 ± 0.009	-21.35 ± 0.35	0.690 ± 0.008	
M	-24.0 ± 1.6	1.302 ± 0.032	-21.33 ± 1.38	1.288 ± 0.026	
L	-32.60 ± 0.67	6.67 ± 0.44	-30.11 ± 0.28 **	6.63 ± 0.36	

391

All the emulsions had relatively stable levels of resveratrol in the oil and aqueous phases during 21-day storage at 4°C (Fig. 5 A-C), suggesting there was no resveratrol degradation or phase migration under refrigeration conditions. The emulsion containing the small droplets also exhibited no detectable change in resveratrol content during storage for three weeks at 37°C (Fig. 5D). Although not statistically significant, there were some observed changes in the partitioning behavior of the resveratrol in the emulsion containing medium droplets during storage at 37 ^{o}C. In particular, the oil phase resveratrol concentration increased from 67.8 ± 3.6% to 79.9 ± 5.5% ($p = 0.063$), while the aqueous phase resveratrol concentration decreased from 32.2 ± 1.5% to 21.5 ± 9.1% over the course of the storage period (Fig. 5E). Notably, no similar pattern was observed for the small or large droplet systems. Notably, the total resveratrol concentration decreased significantly ($p < 0.01$) by 13.2 ± 5.4% after storage for 21 days at 37°C for the emulsion containing the large oil droplets (Fig. 5F).

Overall, these results suggest that the emulsion formulations were highly stable under refrigeration temperatures, but that the resveratrol in the large droplets was susceptible to degradation when stored at higher temperatures. The temperature is a major driver of such processes because of increased molecular mobility, which might be conducive to more rapid exchange between the different phases (Berton-Carabin & Villeneuve, 2023; Robichon et al., 2026). As a result, the resveratrol may spend more time in the aqueous phase, where it is more susceptible to degradation. Moreover, oxidative reactions may be promoted at higher temperatures, leading to thermal degradation of the loaded compound (Zhang et al., 2024). These results suggest that it may be beneficial to store the emulsions under refrigerated conditions and to use smaller oil droplets in emulsion-based delivery systems.

3.3.2 Impact of pH on droplet characteristics and resveratrol stability and partitioning

The chemical stability of resveratrol is known to be strongly influenced by the pH of its surroundings, with rapid degradation occurring under strongly alkaline conditions [3]. For this reason, the impact of aqueous phase pH on the stability of the different resveratrol-loaded emulsions was examined.

Droplet characteristics: There were only relatively small changes in the mean droplet diameters and ζ-potential values of emulsions with different pH values (3-9) after 21 days of storage at 4 or 37 ^{o}C (Table 2), which indicated that the saponin-coated oil droplets were relatively stable to these

conditions. However, there was a slight decrease in the magnitude of the ζ-potential and an increase in the droplet size at the lower pH values. This effect can mainly be attributed to partial protonation of the carboxyl groups on the Quillaja saponin, which reduced the magnitude of the surface charged, thereby weakening the electrostatic repulsion between the droplets.

Table 2: Effects of pH and storage temperature on the ζ-potential and mean particle diameter (D[3,2]) of resveratrol-loaded MCT oil-in-water emulsions. Measurements were taken immediately after preparation (Day 0) and after storage at 4 °C or 37 °C for three weeks (Day 21). Values are expressed as mean ± standard deviation from at least three biological replicates. *p<0.05, **p<0.01

Storage time	*Day 0*		*Day 21 (4°C)*		*Day 21 (37°C)*	
Sample	ζ-potential (mV)	D [3,2] (μm)	ζ-potential (mV)	D [3,2] (μm)	ζ-potential (mV)	D [3,2] (μm)
pH 3			-17.9 ± 1.2 *	0.737 ± 0.043	-18.9 ± 2.3 *	0.724 ±0.003 *
pH 5			-18.4 ± 1.3 **	0.700 ± 0.001	-18.12 ± 0.71 **	0.699 ± 0.002
pH 7	-22.88 ± 0.71	0.689 ± 0.001	-21.33 ± 0.73	0.690 ± 0.006	-19.8 ± 1.7	0.689 ± 0.006
pH 8			-22.4 ± 2.0	0.659 ± 0.008	-22.4 ± 1.0	0.660 ± 0.008
pH 9			-21.0 ± 2.4	0.659 ± 0.007	-22.4 ± 1.2	0.660 ± 0.008

Resveratrol stability under acidic to neutral conditions: When stored at 4° C, all emulsions exhibited good resveratrol stability at pH 3, 5, and 7 (Fig. 6A-C). Indeed, the total resveratrol concentration remained approximately equal to the initial value throughout the 21 days study period and was not significantly different over time ($p > 0.05$). When stored at 37°C, the most acidic emulsions (pH 3 and 5) remained relatively constant in their total resveratrol concentration for 21 days (Fig. 6D, 5E). However, at pH 7 some significant breakdown of resveratrol occurred at 37°C, with the total resveratrol concentration decreasing to 89.78% by day 21 (Fig. 6F). Overall, the partitioning of the resveratrol between the oil and water phases remained relatively constant, although there were some changes. For example, at pH 7, we observed that the resveratrol concentration in the aqueous phase remained relatively stable over time, while that in the oil phase gradually decreased. This observation is in agreement with the findings of Narkiewicz-Michalek et al. (2019), who reported a similar depletion pattern. This indicates that elevated temperature increases the paths of oxidative degradation even when the pH is neutral. Previous researchers

have reported that resveratrol is chemically stable under relatively acidic conditions but chemically degrades around pH 6.8 and higher (Zupančič et al., 2015), which is consistent with our results.

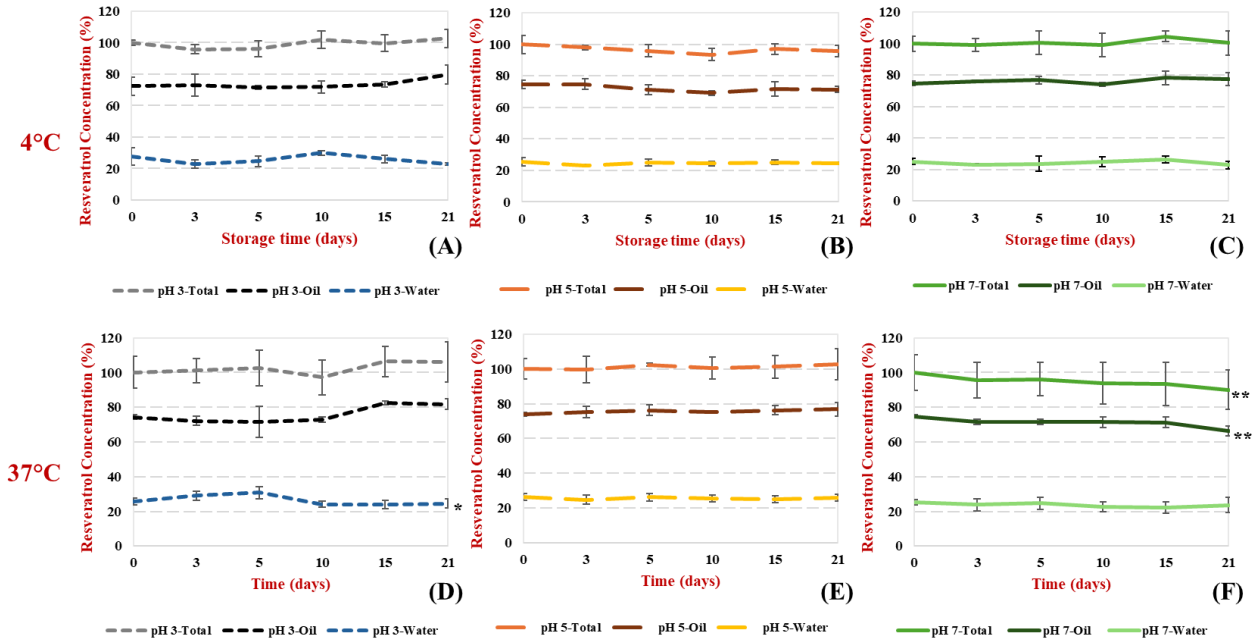


Figure 6: Calculated resveratrol concentration (%) during the 21 days of storage time. The included data show the concentration from the entire emulsion (Total), the aqueous phase (Water), and the oil and surfactant phase (Oil). Small droplet size emulsions with adjusted pH to 3, 5, and 7 were evaluated. The storage temperature was represented by 4°C **(A, B, C)** and 37°C **(D, E, F)**. Values are expressed as mean ± standard deviation from at least three biological replicates. *p<0.05, **p<0.01

Resveratrol degradation under alkaline conditions. In contrast to the relatively good chemical stability of resveratrol observed under acidic and neutral conditions, appreciable resveratrol degradation was observed in the emulsions with higher pH values at both storage temperatures. At 4°C, a significant decrease in the total concentration of resveratrol present was observed at pH 8 ($p < 0.001$). For instance, the total resveratrol concentration present reduced from 100% to 85.8% by day 21 (Fig. 7A), in comparison with the negligible change for pH 7 during that same time period ($p > 0.05$). While the aqueous resveratrol concentration remained stable ($p = 0.489$) at pH 8, resveratrol in the oil phase showed a significant concentration decline (78.0 to 65.2%, $p < 0.001$). The degradation of resveratrol was appreciably faster at pH 8 when the emulsions were stored at

37°C ($p < 0.001$), with the total resveratrol concentration decreasing from 100% to 60.6% after 21 days (Fig. 7C), which was nearly three times higher degradation than observed at 4°C. When stored at 37°C, resveratrol levels in the aqueous and oil phases decreased significantly from 25.4% to 13.1% and from 74.6% to 47.5% ($p < 0.001$), respectively. The accelerated resveratrol degradation with increased pH and temperature suggests a combined effect of the two factors on polyphenol stability. Previous studies have shown that the polyphenolic hydroxyl groups become ionized under alkaline conditions, which increases nucleophilic attacks on the polyphenol backbone (Friedman & Jürgens, 2000).

At pH 9, resveratrol showed extensive degradation at both high and low temperatures, with the rate of degradation being much more severe than that observed at lower pH values. At 4°C, there was a complete loss of resveratrol after only 72 hours of storage. This temperature showed a total loss of resveratrol from the aqueous phase by 24 hours and from the oil phase after 72 hours of storage (Fig. 7B). Increasing the storage temperature to 37°C induced faster degradation, with all the resveratrol being lost after 36 hours of storage (Fig. 7D). After complete degradation occurred, resveratrol quantification was not continued further. The resveratrol content in the water phase at pH 9 seemed to be lower than at the other pH values, but this effect might be attributed to the continuous degradation of the compound during and after extraction. This highlights the extensive degradation of resveratrol in the aqueous phase at such high pH levels, even when encapsulated in oil droplets that were able to protect resveratrol at more neutral pH values.

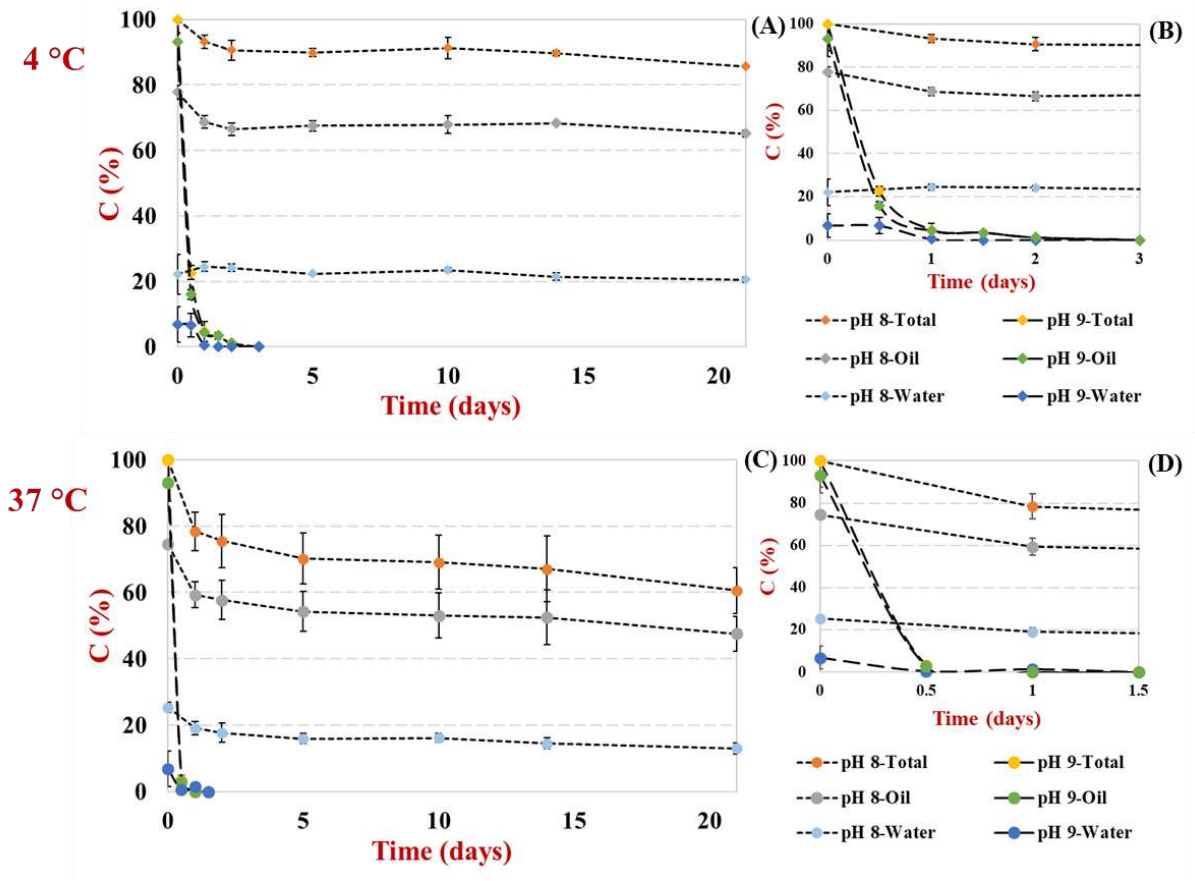


Figure 7: Resveratrol retention in MCT oil-in-water emulsions at pH 8 and pH 9 during 21 days of storage at 4 °C **(A, B)** and 37 °C **(C, D)**. For each condition, the total resveratrol concentration (Total), concentration from the aqueous phase (Water), and from the oil phase (Oil) were analyzed. Plots B and D have different storage time values, which represent the days when pH 9 samples reached total resveratrol degradation. Values are expressed as mean ± standard deviation from at least three biological replicates.

An important factor in resveratrol degradation appears to be its accumulation at the oil–water interface of the emulsion. In this location, the resveratrol is more exposed to the presence of free radicals and oxygen compared to when it is within the bulk oil or aqueous phases of an emulsion (Gong et al., 2022). Studies have shown that resveratrol is substantially partitioned to the oil–water interface of the emulsion, and its impact on the oxidation of the emulsion is also strongest at this location (Narkiewicz-Michalek et al., 2019), providing evidence for an interface-driven degradation of the compound.

The pH-dependent solubility characteristics of resveratrol seem to be closely related to its chemical stability in emulsions, being most stable at acidic to neutral conditions where it is predominantly hydrophobic and least stable under strongly alkaline conditions where it is predominantly hydrophilic (Robinson et al., 2015). Thus, its affinity for the oil phase increases under acidic and neutral environments, which may account for its migration from the aqueous to oil phases, where it is more protected (Zhou et al., 2021b). In contrast, under alkaline conditions it is mainly located in the aqueous phase, where it is more susceptible to chemical degradation.

3.4. UV-light exposure impact on the resveratrol emulsion stability

UV-light exposure is known to accelerate the chemical degradation of resveratrol (Juškaitė et al., 2017), and so we examined the photostability of resveratrol encapsulated within the emulsions. Initially, an infrared thermometer was used to establish the extent of sample heating during the UV light exposure (Fig. 8). The surface temperature of the emulsions was measured during UV irradiation and did not exceed 29 °C, confirming that thermal degradation or evaporation had little to no influence on the results.

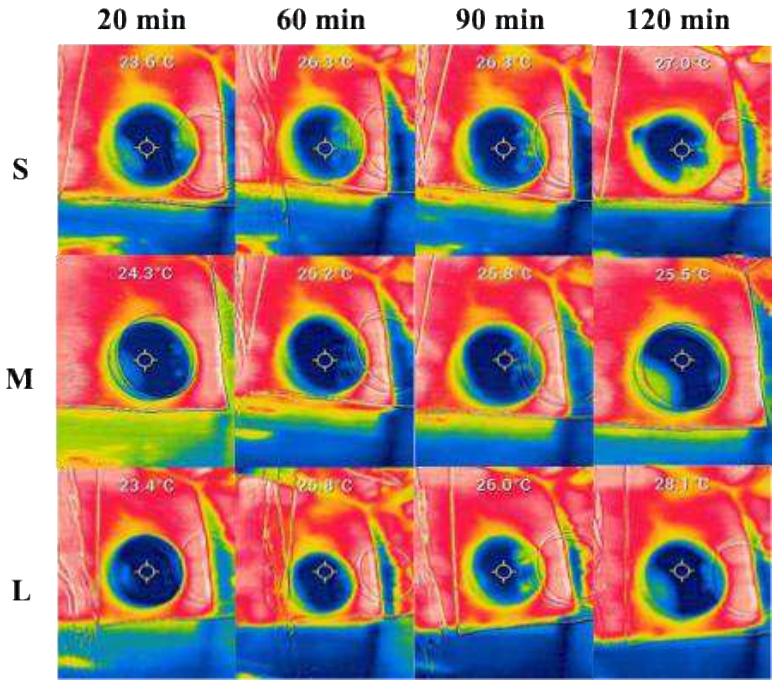


Figure 8: To ensure thermal degradation or evaporation did not influence the recorded data, the temperature on the emulsion surface was measured at 20, 60, 90, and 120 min using an infrared thermometer during UV-light exposure.

3.4.1 Determination of the best model fit

An initial comparison of our experimental data to different kinetic models indicated that resveratrol degradation could be best described by second-order kinetics for all the emulsions. When the reciprocal of resveratrol concentration ($1/C$) was plotted against time, an approximately linear relationship was obtained, which is consistent with the integrated second-order rate law (Section 2.10). Indeed, our analysis found a good correlation between the predicted and observed data for all samples using this model (Tables 3 and 4), with $R^2 > 0.93$ (Simonin, 2016). Using this kinetic model, the influence of droplet size and pH on the photostability of the encapsulated resveratrol was then assessed.

3.4.2 Impact of droplet size on photostability of encapsulated resveratrol

The resveratrol content in the emulsions declined sharply during the first 20 minutes of UV exposure in the three emulsions with different droplets (Fig. 9A). By the end of the exposure period, the resveratrol retention was only 15.2%, 16.8%, and 9.6% of the initial concentration in the emulsions containing small, medium, and large droplets, respectively. As shown in Fig. 9B, the experimental and predicted 1/C versus time profiles were in relatively good agreement, suggesting second-order kinetic degradation.

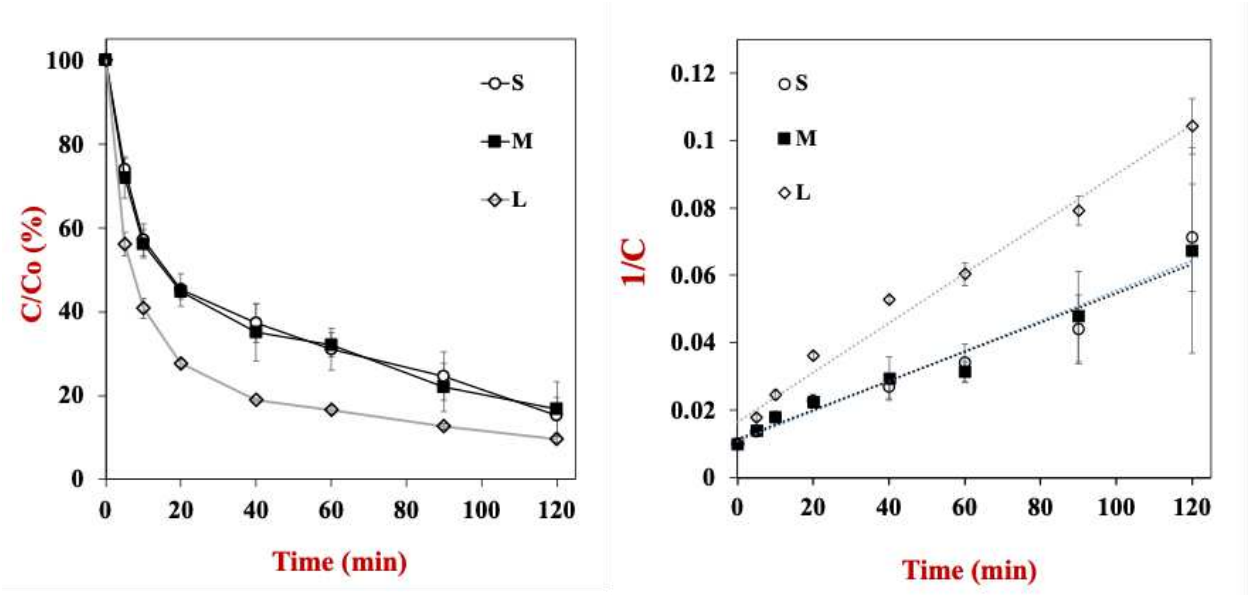


Figure 9. UV degradation kinetics of resveratrol in MCT emulsions containing small (S), medium (M), and large (L) oil droplets: **(A)**. Concentration versus time; (**B**) 1/C versus time (second-order kinetic model). The model provided a reasonable fit across all formulations (R^2 values displayed

in Table 3). Values are expressed as mean ± standard deviation from at least three biological replicates. A linear regression line is fitted to the 1/C versus time data.

The surface charge measured after 120 minutes of UV exposure had lower absolute values than the initial charge for all three emulsions (Table 3). The most pronounced change was observed in the emulsion containing the small droplets, where the ζ-potential changed from -22.9 mV to -14.1 mV ($p < 0.05$). The negative charge on the droplet surfaces can mainly be attributed to the ionizable carboxyl groups on the sugar units of the Quillaja saponin (Reichert et al., 2019). Our results therefore suggest that UV light exposure might compromise not only the resveratrol stability but also the electrostatic barrier provided by this surfactant.

The second-order degradation rate constant (k_2) was highest in the emulsion containing the largest oil droplets, being roughly 1.6× higher than the rate constants obtained for the emulsions containing small or medium droplets (Table 3). The t_{50} values also depended on the droplet size of the emulsions, being 23.3 ± 5.3 min for the small droplets, 26.8 ± 11.6 min for the medium droplets, and 13.6 ± 0.4 min for the large droplets. Although the large droplet emulsion exhibited a higher k_2 and shorter t_{50} than the small and medium droplet emulsions, these differences were not statistically significant ($p > 0.05$). There are several possible reasons for the impact of droplet size on degradation rate. First, as the droplet size decreases, the specific surface area increases, so there may be more resveratrol located at the droplet surfaces (McClements, 2015). The local molecular environment of the resveratrol may then impact its susceptibility to chemical degradation. Second, the size of the oil droplets impacts the extent of ultraviolet light scattering (Choi & McClements, 2020; Davidov-Pardo & McClements, 2015), which may alter the fraction of photons that penetrate into the oil phase where resveratrol is located. Overall, our results suggest that reducing the oil droplet size is an effective strategy for improving the UV photostability of resveratrol in emulsions.

Table 3: Droplet surface potential (ζ-potential) before and after UV light exposure and second-order kinetic parameters for the UV photodegradation of resveratrol in emulsions containing small (S), medium (M), and large (L) oil droplets. Values are expressed as mean ± standard deviation. *$p<0.05$.

Sample	Second order k (min^{-1})	R^2	t_{50}(min)	*Initial ζ-potential (mV)*	*Final ζ-potential (mV)*
S	0.00045 ± 0.0001	0.937 ± 0.065	23.3 ± 5.3	-22.88 ± 0.71	-14.1 ± 1.3 *
M	0.00043 ± 0.0002	0.957 ± 0.041	27 ± 12	-24.0 ± 1.6	-20.7 ± 1.1
L	0.00074 ± 0.0001	0.974 ± 0.007	13.6 ± 0.4	-32.60 ± 0.67	-30.66 ± 0.44 *

568

569 *3.4.3 Impact of pH on photostability of encapsulated resveratrol*

570 To evaluate the impact of pH on the photodegradation of resveratrol under UV exposure,
571 emulsions containing small droplets were adjusted to different pH values and then irradiated with
572 UV for 120 min. There was an appreciable decrease in the resveratrol concentration with exposure
573 time, especially for the most alkaline emulsion (Fig. 10). The degradation of resveratrol at all pH
574 values followed second-order kinetics, with high correlation coefficients ($R^2 > 0.97$) obtained for
575 pH 3, 5, and 7 (Table 4) but less high ones ($R^2 > 0.87$) obtained for pH 8 and pH 9. This effect
576 may be explained by the fact that the chemical degradation of resveratrol can follow additional
577 pathways besides UV photodegradation under strongly alkaline conditions (Zupančič et al., 2015).
578 The divergence in model fit quality between acidic/neutral ($R^2 > 0.97$) and alkaline ($R^2 = 0.87$-
579 0.89) conditions suggests a distinct degradation mechanism when resveratrol is substantially
580 ionized, potentially involving base-catalyzed autoxidation in addition to the UV-driven pathway.
581 Resveratrol loss was generally similar at pH 3, 5, and 7, with resveratrol amounts left after 120
582 minutes being 17.0%, 16.6%, and 14.5% of their initial amounts (Fig. 10A). Surprisingly,
583 resveratrol degradation was slower at pH 8 than under acidic or neutral conditions (lower k_2
584 values), with there being around 21.5% of initial resveratrol left after 120 minutes. In contrast,
585 resveratrol degradation was much more rapid at pH 9 (higher k_2 values), with the amount of
586 resveratrol remaining reduced to only 4.41% of its initial amount after 20 minutes of the UV light
587 experiment (Fig. 10A).

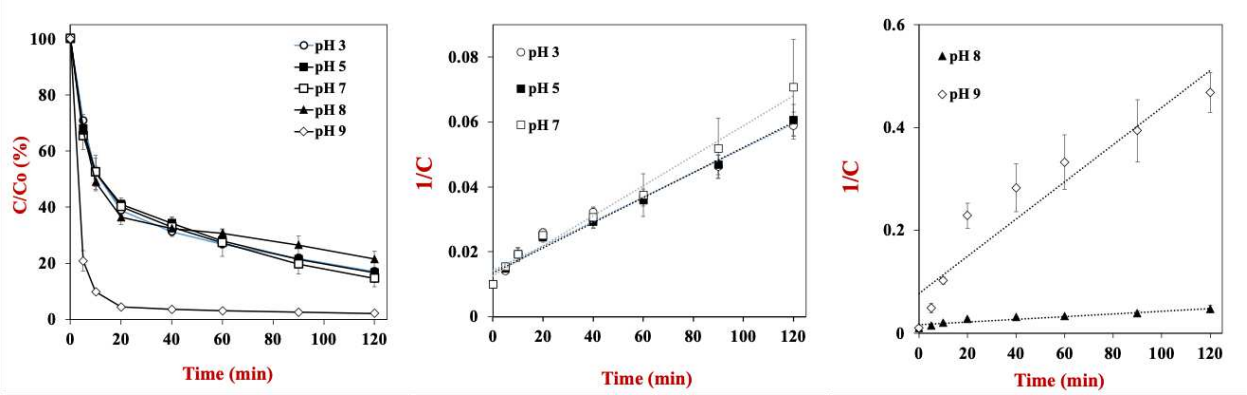


Figure 10: Impact of pH on UV degradation kinetics of resveratrol in MCT emulsions containing small oil droplets: (A). Concentration versus time; (B) 1/C versus time at pH 3, 5, and 7. (B) 1/C versus time at pH 8 and 9. Degradation was much faster under strongly alkaline conditions than under acidic and neutral conditions. Data are shown as mean ± standard deviation.

The ζ-potential values recorded after UV exposure were comparable to the initial value measured at pH 5. However, at pH 3, 5, and 7, the absolute values of the ζ-potential after UV exposure were slightly lower than the initial values ($p < 0.05$). Conversely, at pH 8 and 9, there was no significant change in surface charge after UV exposure ($p > 0.05$), which indicates that the interfacial saponin layer, once chemically altered by alkaline pH (Jiang et al., 2019), becomes less sensitive to UV-induced charge loss. This non-significant data point in response to pH 9 is notable since it was the same pH at which resveratrol decomposed almost entirely within minutes. This implies that the high instability of resveratrol at this pH value was probably caused by the base catalysis of resveratrol decomposition and the compromised protective function of the saponin interfacial film.

The half-lives (t_{50}) of the emulsions containing small oil droplets were 26.7 ± 2.5, 26.0 ± 2.4, and 22.5 ± 5.1 minutes at pH 3, 5, and 7, respectively; rising to 39.0 ± 8.5 minutes at pH 8 and falling to 2.8 ± 0.4 minutes at pH 9 (Table 4). The half-life at pH 9 was therefore much smaller than all other tested pH values ($p < 0.001$). This indicated the near-complete catalysis of trans-resveratrol after a few minutes under the influence of UV light under alkaline conditions. The effect of pH on the second-order rate constant is even more pronounced (Table 4). All conditions are within roughly the same order of magnitude except pH 9, where there is approximately a 7- to 14-fold increase compared to the other four conditions. With the exception of pH 9, the influence of pH on k for pH 3–8 is marginal, where pH 8 is lower compared to pH 3, 5 and 7, but not reaching statistical significance.

Table 4: Second-order kinetic parameters of resveratrol in nanoemulsions at different pH values after UV degradation. Surface charge was analyzed before pH change (Initial ζ-potential) and before UV light exposure experiment (Final ζ-potential). Values are expressed as mean ± standard deviation. *p<0.05

pH value	Second order k (min^{-1})	R^2	t_{50}(min)	*Initial ζ-potential (mV)*	*Final ζ-potential (mV)*
3	0.00038 ± 0.00004	0.971 ± 0.008	26.7 ± 2.5		-15.0 ± 1.2 *
5	0.00039 ± 0.00004	0.985 ± 0.001	26 ± 2.4		-12.5 ± 2.0 *
7	0.00046 ± 0.00011	0.984 ± 0.003	22.5 ± 5.1	-22.88 ± 0.71	-14.9 ± 2.0 *
8	0.00027 ± 0.00007	0.875 ± 0.084	39.0 ± 8.5		-23.03 ± 0.59
9	0.00361 ± 0.00048 *	0.888 ± 0.024	2.8 ± 0.4 *		-20.1 ± 2.8

These findings are consistent with the chemical acid-base characteristics of resveratrol. Resveratrol has phenolic hydroxyl groups with acid dissociation constants (pK_a) values ranging from 8.8 to 9.5 (López-Nicolás & García-Carmona, 2008). When the solution pH exceeds this value, the increasing proportion of deprotonation leads to resveratrol phenolate formation. These forms have significantly higher electron density, as well as greater susceptibility to oxidation and photo-oxidation, compared to the neutral protonated resveratrol present at acidic and neutral pH (Plauth et al., 2016). Improvement in stability at pH 8 compared to acidic and neutral pH, and decrease in stability at pH 9 can be attributed to the pH approaching resveratrol pK_a, where chemical reactivity becomes the dominant factor compared to oil droplet stability.

Considering the formulation perspective, these findings indicate that maintaining the pH of the emulsion neutral or below the pK_a of resveratrol is essential to ensure good photostability under UV radiation. The results underline that pH 9 and higher is the point beyond which resveratrol stability is severely compromised.

4. Conclusion

Our findings show that the stability of resveratrol in MCT oil-in-water emulsions is influenced by a combination of oil droplet size, solution pH, storage temperature, and UV light exposure. A high resveratrol encapsulation efficiency (>93%) was obtained using a simple pH-driven loading

method. The effects of droplet size were examined by preparing emulsions containing small, medium, and large oil droplets. Notably, there was higher resveratrol partitioning into the oil phase for the emulsions containing the smaller oil droplets, which was probably because of their larger specific surface area. Indeed, resveratrol is known to accumulate at oil-water interfaces, suggesting that it has some amphiphilic characteristics, which may impact its stability, release, and efficacy in delivery systems. Most formulations remained physically and chemically stable throughout three weeks of refrigerated storage, although the emulsions containing the largest oil droplets did exhibit appreciable creaming. Even so, the droplets could still be redispersed in these systems by gentle shaking. At 37°C, the resveratrol in the emulsions containing the largest oil droplets degraded most rapidly, while that in the emulsions containing the smallest oil droplets remained largely unchanged. The protective effect of the small droplets may have been due to greater interfacial partitioning of the resveratrol, or due to greater light scattering by the small droplets (thereby reducing the amount of light penetrating into the system).

An important factor influencing the storage stability of encapsulated resveratrol was the pH of the aqueous phase, both during storage and when exposed to UV light. The resveratrol remained relatively stable for emulsions with acidic to neutral aqueous phases (pH 3–7), with only a modest loss being observed during storage at pH 7 and 37°C. In contrast, rapid degradation occurred during storage for emulsions containing alkaline aqueous phases, especially around and above the pK_a value of the resveratrol. At pH 8, resveratrol degradation was significant, while at pH 9 it was rapid, showing considerable losses within days. A similar pH dependence was found for UV photodegradation, where second-order kinetics described the data well at acidic to neutral pH values, and reasonably well under alkaline conditions. Smaller droplets offered better photoprotection than larger ones, which was mainly attributed to greater scattering of ultraviolet light waves by smaller droplets, thereby reducing photon penetration.

Overall, these results show that smaller droplet size, mildly acidic to neutral pH, refrigerated storage, and low light conditions are the most effective for preserving resveratrol in emulsion-based delivery systems. These guidelines should be useful for developing resveratrol-loaded delivery systems for functional foods, beverages, and cosmeceutical applications. More broadly, the principles we identified, particularly the roles of resveratrol partitioning and pH-dependent ionization, might also apply to other lipophilic, pH-sensitive polyphenols in oil-in-water emulsions. Further work could be performed to identify the degradation products generated under

alkaline and UV-stress conditions, as well as to assess how these optimized formulations perform regarding their sensory properties, bioavailability, bioactivity, and safety.

Acknowledgments

The first author would like to thank the Romanian-US Fulbright Commission for the financial support.

References

Berman, A. Y., Motechin, R. A., Wiesenfeld, M. Y., & Holz, M. K. (2017). The therapeutic potential of resveratrol: A review of clinical trials. *Npj Precision Oncology*, *1*(1), 35. https://doi.org/10.1038/s41698-017-0038-6

Bertoldo, A., Pizzol, D., Yon, D. K., Callegari, M., Gobbo, V., Cuccurese, P., Butler, L., Caminada, S., Stebbing, J., Richardson, F., Gawronska, J., & Smith, L. (2024). Resveratrol and Female Fertility: A Systematic Review. *International Journal of Molecular Sciences*, *25*(23), 12792. https://doi.org/10.3390/ijms252312792

Berton-Carabin, C., & Villeneuve, P. (2023). Targeting Interfacial Location of Phenolic Antioxidants in Emulsions: Strategies and Benefits. *Annual Review of Food Science and Technology*, *14*(1), 63–83. https://doi.org/10.1146/annurev-food-060721-021636

Bonto, M., Eftekhari, A. A., & Nick, H. M. (2019). An overview of the oil-brine interfacial behavior and a new surface complexation model. *Scientific Reports*, *9*(1), 6072. https://doi.org/10.1038/s41598-019-42505-2

Chen, Y., Cheng, H., & Liang, L. (2023). Effect of Oil Type on Spatial Partition of Resveratrol in the Aqueous Phase, the Protein Interface and the Oil Phase of O/W Emulsions Stabilized by Whey Protein and Caseinate. *Antioxidants*, *12*(3), 589. https://doi.org/10.3390/antiox12030589

Choi, S. J., & McClements, D. J. (2020). Nanoemulsions as delivery systems for lipophilic nutraceuticals: Strategies for improving their formulation, stability, functionality and bioavailability. *Food Science and Biotechnology*, *29*(2), 149–168. https://doi.org/10.1007/s10068-019-00731-4

Cvejić, J., Poša, M., Sebenji, A., & Atanacković, M. (2014). Comparison of Solubilization Capacity of Resveratrol in Sodium 3 α ,12 α -Dihydroxy-7-oxo-5 β -cholanoate and Sodium Dodecyl Sulfate. *The Scientific World Journal*, *2014*, 1–7. https://doi.org/10.1155/2014/265953

Daszkiewicz, T., Florek, M., Murawska, D., & Jabłońska, A. (2024). A comparison of the quality of ultra-high-temperature milk and its plant-based analogs. *Journal of Dairy Science*, *107*(12), 10299–10309. https://doi.org/10.3168/jds.2024-25098

Davidov-Pardo, G., & McClements, D. J. (2015). Nutraceutical delivery systems: Resveratrol encapsulation in grape seed oil nanoemulsions formed by spontaneous emulsification. *Food Chemistry*, *167*, 205–212. https://doi.org/10.1016/j.foodchem.2014.06.082

Friedman, M., & Jürgens, H. S. (2000). Effect of pH on the Stability of Plant Phenolic Compounds. *Journal of Agricultural and Food Chemistry*, *48*(6), 2101–2110. https://doi.org/10.1021/jf990489j

Golding, M., & Wooster, T. J. (2010). The influence of emulsion structure and stability on lipid digestion. *Current Opinion in Colloid & Interface Science*, *15*(1–2), 90–101. https://doi.org/10.1016/j.cocis.2009.11.006

706 Gong, T., Chen, B., Hu, C. Y., Guo, Y. R., Shen, Y. H., & Meng, Y. H. (2022). Resveratrol inhibits lipid
707 and protein co-oxidation in sodium caseinate-walnut oil emulsions by reinforcing oil-water
708 interface. *Food Research International*, *158*, 111541.
709 https://doi.org/10.1016/j.foodres.2022.111541

710 Ho, Y. (2006). Review of second-order models for adsorption systems. *Journal of Hazardous Materials*,
711 *136*(3), 681–689. https://doi.org/10.1016/j.jhazmat.2005.12.043

712 Hu, L., Wu, L., Lai, C., Li, M., & Yang, W. (2022). The influence of pH and concentration on the zeta
713 potential, hydrophobicity of OVT and the relationship between its structure and interfacial
714 behaviors. *Journal of Dispersion Science and Technology*, *43*(12), 1755–1765.
715 https://doi.org/10.1080/01932691.2021.1880431

716 Hu, Q., & Zhang, Z. (2020). Prediction of half-life for adsorption kinetics in a batch reactor. *Environmental*
717 *Science and Pollution Research*, *27*(35), 43865–43869. https://doi.org/10.1007/s11356-020-
718 10228-x

719 Hung, C.-F., Chen, J.-K., Liao, M.-H., Lo, H.-M., & Fang, J.-Y. (2006). Development and Evaluation of
720 Emulsion-Liposome Blends for Resveratrol Delivery. *Journal of Nanoscience and*
721 *Nanotechnology*, *6*(9), 2950–2958. https://doi.org/10.1166/jnn.2006.420

722 Jiang, X., Strobel, B. W., Cedergreen, N., Cao, Y., & Hansen, H. Chr. B. (2019). Stability of saponin
723 biopesticides: Hydrolysis in aqueous solutions and lake waters. *Environmental Science: Processes*
724 *& Impacts*, *21*(7), 1204–1214. https://doi.org/10.1039/C9EM00012G

725 Jiang, X., Zuo, L., Gao, S., Yang, Q., Li, Y., Chen, Y., Xie, X., & Peng, C. (2025). Green Production
726 Pathways, Instability, and Stability of Resveratrol: A Systematic Review. *Journal of Food*
727 *Biochemistry*, *2025*(1). https://doi.org/10.1155/jfbc/8210896

728 Juškaitė, V., Ramanauskienė, K., & Briedis, V. (2017). Testing of resveratrol microemulsion photostability
729 and protective effect against UV induced oxidative stress. *Acta Pharmaceutica*, *67*(2), 247–256.
730 https://doi.org/10.1515/acph-2017-0018

731 Kasiotis, K. M., Pratsinis, H., Kletsas, D., & Haroutounian, S. A. (2013). Resveratrol and related stilbenes:
732 Their anti-aging and anti-angiogenic properties. *Food and Chemical Toxicology*, *61*, 112–120.
733 https://doi.org/10.1016/j.fct.2013.03.038

734 Khan, S., Zahiruddin, S., Khan, A. H., & Ahmad, S. (2025). Exploring the Nutritional and Antioxidant
735 Potential of a Developed Fusion: Coconut Water and Orange Juice Beverage. *Journal of Food*
736 *Quality*, *2025*(1). https://doi.org/10.1155/jfq/7286503

737 Kharat, M., Aberg, J., Dai, T., & McClements, D. J. (2020). Comparison of Emulsion and Nanoemulsion
738 Delivery Systems: The Chemical Stability of Curcumin Decreases as Oil Droplet Size Decreases.
739 *Journal of Agricultural and Food Chemistry*, *68*(34), 9205–9212.
740 https://doi.org/10.1021/acs.jafc.0c01877

741 Kotta, S., Mubarak Aldawsari, H., Badr-Eldin, S. M., Alhakamy, N. A., & Md, S. (2021). Coconut oil-
742 based resveratrol nanoemulsion: Optimization using response surface methodology, stability
743 assessment and pharmacokinetic evaluation. *Food Chemistry*, *357*, 129721.
744 https://doi.org/10.1016/j.foodchem.2021.129721

745 Li, Y., Li, R., Han, G., Li, B., Xu, Z., Pan, S., & Liu, F. (2024). Effect of oil phase type and lutein loading
746 on emulsifying properties and in vitro digestion of mandarin peel pectin emulsions. *LWT*, *194*,
747 115799. https://doi.org/10.1016/j.lwt.2024.115799

748 Li, Y., & McClements, D. J. (2010). New Mathematical Model for Interpreting pH-Stat Digestion Profiles:
749 Impact of Lipid Droplet Characteristics on in Vitro Digestibility. *Journal of Agricultural and Food*
750 *Chemistry*, *58*(13), 8085–8092. https://doi.org/10.1021/jf101325m

López-Nicolás, J. M., & García-Carmona, F. (2008). Aggregation State and p K_a Values of (E)-Resveratrol As Determined by Fluorescence Spectroscopy and UV−Visible Absorption. *Journal of Agricultural and Food Chemistry*, *56*(17), 7600–7605. https://doi.org/10.1021/jf800843e

Losada-Barreiro, S., Costa, M., Bravo-Díaz, C., & Paiva-Martins, F. (2014). Distribution and Antioxidant Efficiency of Resveratrol in Stripped Corn Oil Emulsions. *Antioxidants*, *3*(2), 212–228. https://doi.org/10.3390/antiox3020212

McClements, D. J. (2015). *Food Emulsions: Principles, Practices, and Techniques, Third Edition* (0 ed.). CRC Press. https://doi.org/10.1201/b18868

Meng, T., Xiao, D., Muhammed, A., Deng, J., Chen, L., & He, J. (2021). Anti-Inflammatory Action and Mechanisms of Resveratrol. *Molecules*, *26*(1), 229. https://doi.org/10.3390/molecules26010229

Meynier, A., Lecoq, C., & Genot, C. (2005). Emulsification enhances the retention of esters and aldehydes to a greater extent than changes in the droplet size distribution of the emulsion. *Food Chemistry*, *93*(1), 153–159. https://doi.org/10.1016/j.foodchem.2004.10.018

Miadonye, A., & Amadu, M. (2023). Theoretical Interpretation of pH and Salinity Effect on Oil-in-Water Emulsion Stability Based on Interfacial Chemistry and Implications for Produced Water Demulsification. *Processes*, *11*(8), 2470. https://doi.org/10.3390/pr11082470

Narkiewicz-Michalek, J., Szymula, M., Losada-Barreiro, S., & Bravo-Diaz, C. (2019). Concentration of resveratrol at the oil–water interface of corn oil-in-water emulsions. *Adsorption*, *25*(4), 903–911. https://doi.org/10.1007/s10450-019-00108-3

Nimbkar, S., Leena, M. M., Moses, J. A., & Anandharamakrishnan, C. (2022). Medium chain triglycerides (MCT): State-of-the-art on chemistry, synthesis, health benefits and applications in food industry. *Comprehensive Reviews in Food Science and Food Safety*, *21*(2), 843–867. https://doi.org/10.1111/1541-4337.12926

Plauth, A., Geikowski, A., Cichon, S., Wowro, S. J., Liedgens, L., Rousseau, M., Weidner, C., Fuhr, L., Kliem, M., Jenkins, G., Lotito, S., Wainwright, L. J., & Sauer, S. (2016). Data of oxygen- and pH-dependent oxidation of resveratrol. *Data in Brief*, *9*, 433–437. https://doi.org/10.1016/j.dib.2016.09.012

Reddy, A., Norris, D. F., Momeni, S. S., Waldo, B., & Ruby, J. D. (2016). The pH of beverages in the United States. *The Journal of the American Dental Association*, *147*(4), 255–263. https://doi.org/10.1016/j.adaj.2015.10.019

Reichert, C. L., Salminen, H., & Weiss, J. (2019). *Quillaja* Saponin Characteristics and Functional Properties. *Annual Review of Food Science and Technology*, *10*(1), 43–73. https://doi.org/10.1146/annurev-food-032818-122010

Robichon, C., Durand, E., Gamaethiralalage, J. G., Bohuon, P., Baréa, B., Barouh, N., Courtois, F., Fine, F., De Smet, L. C. P. M., & Villeneuve, P. (2026). Decoding Tocopherol–Polyphenol interactions in oil-in-water emulsions through combined WIM-CAT and CV assays. *Current Research in Food Science*, *12*, 101344. https://doi.org/10.1016/j.crfs.2026.101344

Robinson, K., Mock, C., & Liang, D. (2015). Pre-formulation studies of resveratrol. *Drug Development and Industrial Pharmacy*, *41*(9), 1464–1469. https://doi.org/10.3109/03639045.2014.958753

Shi, R., Gao, D., Stoika, R., Liu, K., Sik, A., & Jin, M. (2024). Potential implications of polyphenolic compounds in neurodegenerative diseases. *Critical Reviews in Food Science and Nutrition*, *64*(16), 5491–5514. https://doi.org/10.1080/10408398.2022.2155106

Simonin, J.-P. (2016). On the comparison of pseudo-first order and pseudo-second order rate laws in the modeling of adsorption kinetics. *Chemical Engineering Journal*, *300*, 254–263. https://doi.org/10.1016/j.cej.2016.04.079

Su, M., Zhao, W., Xu, S., & Weng, J. (2022). Resveratrol in Treating Diabetes and Its Cardiovascular Complications: A Review of Its Mechanisms of Action. *Antioxidants*, *11*(6), 1085. https://doi.org/10.3390/antiox11061085

Taha, A., Hu, T., Zhang, Z., Bakry, A. M., Khalifa, I., Pan, S., & Hu, H. (2018). Effect of different oils and ultrasound emulsification conditions on the physicochemical properties of emulsions stabilized by soy protein isolate. *Ultrasonics Sonochemistry*, *49*, 283–293. https://doi.org/10.1016/j.ultsonch.2018.08.020

Talib, W. H., Alsayed, A. R., Farhan, F., & Al Kury, L. T. (2020). Resveratrol and Tumor Microenvironment: Mechanistic Basis and Therapeutic Targets. *Molecules*, *25*(18), 4282. https://doi.org/10.3390/molecules25184282

Ten Klooster, S., Boerkamp, V. J. P., Hennebelle, M., Van Duynhoven, J. P. M., Schroën, K., & Berton-Carabin, C. C. (2024). Unravelling the effect of droplet size on lipid oxidation in O/W emulsions by using microfluidics. *Scientific Reports*, *14*(1), 8895. https://doi.org/10.1038/s41598-024-59170-9

Ulaganathan, V., Del Castillo, L., Webber, J. L., Ho, T. T. M., Ferri, J. K., Krasowska, M., & Beattie, D. A. (2019). The influence of pH on the interfacial behaviour of Quillaja bark saponin at the air-solution interface. *Colloids and Surfaces B: Biointerfaces*, *176*, 412–419. https://doi.org/10.1016/j.colsurfb.2019.01.017

Zhang, W., Meng, L., Lv, X., Wang, L., Zhao, P., Wang, J., Zhang, X., Chen, J., & Wu, Z. (2024). Enhancing Stability and Antioxidant Activity of Resveratrol-Loaded Emulsions by Ovalbumin–Dextran Conjugates. *Foods*, *13*(8), 1246. https://doi.org/10.3390/foods13081246

Zhao, Q., Lu, C., Chang, C., Gu, L., Li, J., Guo, L., Hu, S., Huang, Z., Yang, Y., & Su, Y. (2024). Studies on the Properties and Stability Mechanism of Double Emulsion Gels Prepared by Heat-Induced Aggregates of Egg White Protein-Oligosaccharides Glycosylation Products. *Foods*, *13*(12), 1822. https://doi.org/10.3390/foods13121822

Zheng, B., Peng, S., Zhang, X., & McClements, D. J. (2018). Impact of Delivery System Type on Curcumin Bioaccessibility: Comparison of Curcumin-Loaded Nanoemulsions with Commercial Curcumin Supplements. *Journal of Agricultural and Food Chemistry*, *66*(41), 10816–10826. https://doi.org/10.1021/acs.jafc.8b03174

Zheng, X., Chu, X., & Pan, H. (2025). Optimization of Encapsulation Core–Shell Structure to Preserve Polyphenols in Soy Protein—Polysaccharide Co-Dried Complexes. *Molecules*, *30*(5), 978. https://doi.org/10.3390/molecules30050978

Zhou, H., Zheng, B., & McClements, D. J. (2021a). Encapsulation of lipophilic polyphenols in plant-based nanoemulsions: Impact of carrier oil on lipid digestion and curcumin, resveratrol and quercetin bioaccessibility. *Food & Function*, *12*(8), 3420–3432. https://doi.org/10.1039/d1fo00275a

Zhou, H., Zheng, B., & McClements, D. J. (2021b). *In Vitro* Gastrointestinal Stability of Lipophilic Polyphenols is Dependent on their Oil–Water Partitioning in Emulsions: Studies on Curcumin, Resveratrol, and Quercetin. *Journal of Agricultural and Food Chemistry*, *69*(11), 3340–3350. https://doi.org/10.1021/acs.jafc.0c07578

Zhou, H., Zheng, B., & McClements, D. J. (2024). Utilization of pH-driven methods to fortify nanoemulsions with multiple polyphenols. *Food Science and Human Wellness*, *13*(4), 1943–1950. https://doi.org/10.26599/FSHW.2022.9250161

Zupančič, Š., Lavrič, Z., & Kristl, J. (2015). Stability and solubility of trans-resveratrol are strongly influenced by pH and temperature. *European Journal of Pharmaceutics and Biopharmaceutics*, *93*, 196–204. https://doi.org/10.1016/j.ejpb.2015.04.002

1. C. Reichert, H. Salminen and J. Weiss, in *Annual Review of Food Science and Technology, Vol 10*, edited by M. P. Doyle and D. J. McClements (2019), Vol. 10, pp. 43–73.
2. M. Kharat, J. Aberg, T. Dai and D. McClements, Journal of Agricultural and Food Chemistry **68** (34), 9205–9212 (2020).
3. K. Robinson, C. Mock and D. Liang, Drug Dev Ind Pharm **41** (9), 1464–1469 (2015).